Propagation effects of low frequency electromagnetic waves in production well

Song Xijin[1, 2*], Guo Baolong[1], Dang Ruirong[2] and Wang Xuelong[3]

[1] Institute of Intelligent Control and Image Engineering, Xidian University, Shaanxi 710071, China
[2] Key Laboratory of Photoelectric Logging and Detecting of Oil and Gas, Ministry of Education, Xi'an Shiyou University, Shaanxi 710065, China
[3] College of Computer Science & Technology, Shaanxi University of Technology, Shaanxi 710048, China

Abstract: The frequency domain electromagnetic method has already been widely used for tomographic imaging or electromagnetic well logging. However, different from open hole logging, the metal casing existing in production well logging has a strong shielding effect on the electromagnetic waves, thus bringing some difficulties to the application of the frequency domain electromagnetic method in production well logging. According to the relation of the field source geometry to the ring around the mandrel, the general expressions of frequency domain electromagnetic responses in axially symmetrical layered conductive medium are deduced. The propagation effects caused by the low-frequency electromagnetic waves in cased hole are also analyzed. The distribution curves of eddy current density and magnetic flux density along the radial direction in the mandrel indicate that the eddy loss within the mandrel is proportional to the transmission signal frequency and the mandrel conductivity. The secondary field responses of different casing materials show that the transmission frequency has an important effect on the ability of electromagnetic waves penetrating the metal casing. The transmission frequency should be ultra-low in order to enable the electromagnetic signal to penetrate the casing easily. The numerical results of frequency responses for different casing physical parameters show that the casing thickness has a significant impact on the choice of the transmission frequency. It is also found that the effect of the casing radius on the transmission frequency can be neglected.

Key words: Propagation effects, eddy current density, magnetic flux density, production well, frequency response

1 Introduction

With the advancement of oilfield exploitation, the oil production capacity of wells is gradually decreasing and the water content is higher and higher. Therefore, the review and tapping of old wells is an essential complement to keeping the stability of oil and gas production. Moreover, it is also an effective way to enhance the overall effect of oilfield development. In view of the large number of cased holes in old wells and the wells which are being exploited, developing through-casing resistivity characteristic identification techniques is urgently needed (Fondyga et al, 2004). Currently, through-casing resistivity logging has become an important means of monitoring old wells and the production process. In addition, the theory of cased hole formation resistivity logging and the calculation of apparent resistivity is extensively studied (Askey et al, 2002; Gao et al, 2008a). In 1939, L. M. Alpin applied for the first patent

about the formation resistivity measurement through casing in the United States. Since then, researchers in the United States, France, Russia and other countries have been actively studying the measurement of formation resistivity through casing (Kaufman, 1990; Kaufman and Wightman, 1993; Vail, 1991; 1993a; 1993b). In 1988, U.S. Paramagnetic Logging successfully tested the first prototype of through-casing resistivity logging according to the patent applied for by Kaufman A A and Vail W B. Kaufman published the cased hole resistivity logging approximation model and the measurement theory based on the transmission line equation, which laid a solid foundation for through-casing resistivity logging (Kaufman, 1990; Kaufman and Wightman, 1993). In 1994, Schenkel and Morrison published a theoretical model based on integral equations, and discussed the logging response caused by a limited length pipe filled with fluid in a radial inhomogeneous medium (Schenkel and Morrison, 1994). The effects of casing thickness and cement sheath on the measurement results were also studied, which enriched and improved the basic theory of through-casing resistivity logging. For the electromagnetic measurement excited outside

*Corresponding author. email: sxj3029@126.com

the cased well and received within it, Xu and Habashy (1994) analyzed the characteristics of attenuation and phase shift of electromagnetic signals inside and outside the casing when excited by a coil of large radius outside the casing, providing a theoretical basis for quantitative interpretation of the electromagnetic measurement through casing. The Schlumberger Company began to put the through-casing resistivity logging device (CHFR—Cased Hole Formation Resistivity) into commercial applications in 2000. In 2006, Russia also completed the development of a through-casing resistivity logging tool and actual measurements in the Liaohe and Daqing oilfields in China (Xue et al, 2006; Bao et al, 2010).

However, compared with through-casing resistivity logging, people pay relatively less attention to the electromagnetic logging in cased holes, mainly because the metal casing has a strong shielding effect on electromagnetic signals, and brings great difficulties to the transmitting and receiving of electromagnetic signals (Che and Qiao, 2009). Furthermore, the propagation of electromagnetic waves in a homogeneous medium may produce amplitude attenuation and phase shift (Kang et al, 2006; Shen and Sun, 2008; Gao et al, 2008b; Wang, 2009); in inhomogeneous medium, due to the presence of the medium interface, it may cause reflection and refraction, i.e. propagation effects. Almost all high-frequency electromagnetic signals are absorbed by the casing and can not enter the formation, but some low-frequency electromagnetic signals can enter formation through the casing and can excite eddy currents. In a non-contact way, the low-frequency electromagnetic method in a borehole can identify the formation resistivity distribution by detecting the electromagnetic response in the receiver coil caused by eddy currents. Both the source and the receiver are located in the borehole, which makes the measuring device closer to the anomalous body. Therefore, the abnormal response signals are increased. The abnormal body can be detected in different heights and from each side. It can be used to study the connectivity of sand bodies, monitor flooding situations and study the distribution of remaining oil, and has a good prospect in oil and gas exploration. Based on the actual work characteristics of oil and gas production well, we derive the general expression of low frequency electromagnetic logging response in a cylindrical layered medium, and analyze the propagation effects caused by the low-frequency electromagnetic waves in a multi-layer conductive medium. The electromagnetic response characteristics in the mandrel and formation are also discussed in detail. The results in this paper can provide an important theoretical basis for the forward modeling, inversion and interpretation of low-frequency electromagnetic logging in production wells.

2 Field equations and their solutions

Low frequency electromagnetic logging methods in production wells use a coil around a mandrel as the source. Fig. 1 shows the schematic diagram. Both the transmitting coil T and the receiving coil R are around a mandrel in borehole. The vertical offset between the two coils is z. Mandrel, hole, casing and formation have conductivity $\{\sigma_1, \sigma_2, \sigma_3, \sigma_4\}$,

permittivity $\{\varepsilon_1, \varepsilon_2, \varepsilon_3, \varepsilon_4\}$ and permeability $\{\mu_1, \mu_2, \mu_3, \mu_4\}$. There are three cylindrical interfaces in cylindrical layered medium shown in Fig. 1, that is mandrel, borehole and casing. Their outer-radii are r, r_1 and r_2, respectively. The basic principle of low-frequency electromagnetic method in cased hole is the law of electromagnetic induction. When we apply low frequency alternating current to the transmitting coil, the electromagnetic field caused by the current would enter the formation though the casing, and produce eddy currents coaxial with the transmitting coil. This eddy further generates induced electromotive force (EMF) in the receiver. So we can determine the formation resistivity characteristics by the response signals. We described the fundamentals of time-domain electromagnetic logging in boreholes previously (Song et al, 2011). The results indicated that compared with metal casing, the impact of a cement sheath on electromagnetic signals is small, and can be neglected especially for low resistance formation. Therefore, in order to simplify the model shown in Fig. 1, we do not consider the cement sheath.
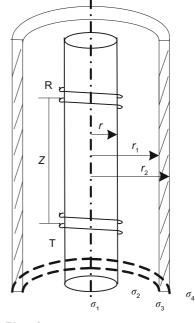

Fig. 1 The schematic of low frequency electromagnetic logging in a production well

2.1 Field of conductive homogeneous medium

To solve the boundary value problems of electromagnetic fields in a homogeneous medium, we need to obtain particular solution items of the non-homogeneous wave equation in the active region. This particular solution is the primary field produced by the source, which is equivalent to the field generated by the source in a uniform infinite medium. In Fig. 1, we define that the transmitting coil is located at $z=z_0$ in the borehole axis and has the radius ρ_0. So the physical model shown in Fig. 1 has axial symmetry, i.e. $\dfrac{\partial}{\partial \varphi}=0$. The field source geometry of the ring current source (transmitting coil) is shown in Fig. 2. Here, the ring current source is regarded as a combination of an infinite number of electric dipole sources, so the electromagnetic field caused by it is the superposition

of an infinite number of fields produced by the electric dipoles. In Fig. 2, a current loop is located at $r_0=(\rho_0, \varphi_0)$, and the current source with an arc length of $\mathrm{d}l$ is an electric dipole. Then the electric dipole source is perpendicular to the meridian plane of the azimuth φ_0, and points to the direction e_{φ_0}. When we apply current $I=I_0e^{i\omega t}$ to the ring current source, the magnetic vector potential meets the Helmholtz equation as follows:

$$\nabla^2 A + k^2 A = -I\mathrm{d}l\delta(r) \qquad (1)$$

where, $\delta(r)$ is the Dirac function. In cylindrical coordinates, the magnetic vector potential components in the azimuth direction e_φ are given by:

$$\mathrm{d}A_\varphi = \frac{I\mathrm{d}l}{4\pi}\frac{e^{-ikR}}{R}\cos(\varphi-\varphi_0) \qquad (2)$$

According to $\mathrm{d}l = \rho_0\mathrm{d}\varphi = \rho_0\mathrm{d}(\varphi-\varphi_0)$, Eq. (2) becomes:

$$\mathrm{d}A_\varphi = \frac{I\rho_0}{4\pi}\frac{e^{-ikR}}{R}\cos(\varphi-\varphi_0)\mathrm{d}(\varphi-\varphi_0) \qquad (3)$$

By integrating Eq. (3) one circle from φ_0, the total magnetic vector potential of the primary field caused by the ring current source is:

$$A_\varphi = \frac{I\rho}{2\pi^2}\int_0^{2\pi}\cos(\varphi-\varphi_0)\mathrm{d}(\varphi-\varphi_0)$$
$$\times\int_0^\infty K_0(\lambda|\rho-\rho_0|)\cos\gamma(z-z_0)\mathrm{d}\gamma \qquad (4)$$

where, $\lambda = \sqrt{\gamma^2-k^2}$. γ is the integral parameter introduced to solve the electromagnetic response. Wave number $k = \sqrt{-i\omega\mu\sigma}$. μ, ε, σ are magnetic permeability, permittivity and conductivity of uniform formation, respectively. Under the modified Bessel function addition formula and the orthogonality of trigonometric functions, Eq. (4) becomes:

$$A_\varphi = \begin{cases} \dfrac{I\rho_0}{\pi}\displaystyle\int_0^\infty I_1(\lambda\rho_0)K_1(\lambda\rho)\cos\gamma(z-z_0)\mathrm{d}\gamma & (\rho > \rho_0) \\ \dfrac{I\rho_0}{\pi}\displaystyle\int_0^\infty I_1(\lambda\rho)K_1(\lambda\rho_0)\cos\gamma(z-z_0)\mathrm{d}\gamma & (\rho < \rho_0) \end{cases} \qquad (5)$$

where, $I_1(\lambda\rho)$ and $K_1(\lambda\rho)$ are modified Bessel functions. By the relationship of vector magnetic potential and electric field strength:

$$E = -i\omega\mu A + \frac{1}{\sigma+i\omega\varepsilon}\nabla\nabla\cdot A \qquad (6)$$

We know that the primary electric field generated by the coil has a component only in direction φ, that is:

$$E_\varphi^{(1)} = \begin{cases} \displaystyle\int_0^\infty gK_1(\lambda\rho)\cos\gamma(z-z_0) & (\rho > \rho_0) \\ \displaystyle\int_0^\infty gI_1(\lambda\rho)\cos\gamma(z-z_0) & (\rho < \rho_0) \end{cases} \qquad (7)$$

where,

$$g = \begin{cases} -\dfrac{i\omega\mu I\rho_0}{\pi}I_1(\lambda\rho_0) & (\rho > \rho_0) \\ -\dfrac{i\omega\mu I\rho_0}{\pi}K_1(\lambda\rho_0) & (\rho < \rho_0) \end{cases} \qquad (8)$$
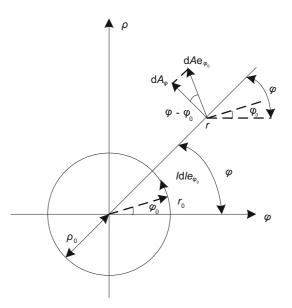

Fig. 2 The field source geometry of the ring current source

2.2 Field in a layered lossy medium

For the axially symmetric model, the eddy induced by the primary electric field only has a component in direction φ. So the secondary electric field in a layered medium also only has a component in direction φ, which meets the passive Helmholtz equation as follows:

$$\nabla^2 E + k^2 E = 0 \qquad (9)$$

In cylindrical coordinate system, Eq. (9) becomes:

$$e_\rho(\nabla^2 E_\varphi - \frac{2}{\rho^2}\frac{\partial E_\varphi}{\partial\varphi} - \frac{E_\varphi}{\rho^2}) + e_\varphi(\nabla^2 E_\varphi + \frac{2}{\rho^2}\frac{\partial E_\varphi}{\partial\varphi} - \frac{E_\varphi}{\rho^2})$$
$$+ e_z\frac{\partial^2 E_z}{\partial z^2} + k^2 E = 0 \qquad (10)$$

The solution to Eq. (10) is the linear combination of the first and second modified Bessel functions. Using separation of variables, and considering that the field is symmetric to the plane $z = z_0$, the secondary electric response is as follows:

$$E_\varphi^{(2)} = \int_0^\infty [AI_1(\lambda\rho) + BK_1(\lambda\rho)]\cos\gamma(z-z_0)\mathrm{d}\gamma \qquad (11)$$

For the model shown in Fig. 1, the general solution in the borehole should be the superposition of the primary field and the secondary field. Other layered media are all passive, then the general solution only has the secondary field response. Therefore, the electric field responses in a four layered medium are as follows:

$$\begin{cases} E_{1\varphi} = \int_0^\infty A_1 I_1(\lambda_1\rho)\cos\gamma(z-z_0)\mathrm{d}\gamma \\[2mm] E_{2\varphi} = \int_0^\infty [-\dfrac{i\omega\mu_2 I\rho_0}{\pi}K_1(\lambda_2\rho_0)I_1(\lambda_2\rho)+A_2 I_1(\lambda_2\rho) \\[2mm] \qquad\quad +B_2 K_1(\lambda_2\rho)]\cos\gamma(z-z_0)\mathrm{d}\gamma \\[2mm] E_{3\varphi} = \int_0^\infty [A_3 I_1(\lambda_3\rho)+B_3 K_1(\lambda_3\rho)]\cos\gamma(z-z_0)\mathrm{d}\gamma \\[2mm] E_{4\varphi} = \int_0^\infty B_4 K_1(\lambda_4\rho)\cos\gamma(z-z_0)\mathrm{d}\gamma \end{cases} \quad (12)$$

By the relationship of the magnetic potential vector and the magnetic field strength:

$$H = \nabla \times A \tag{13}$$

the magnetic field in the tangential direction at the cylindrical interface is:

$$H_z = -\frac{1}{i\omega\mu}\left(\frac{E_\varphi}{r}+\frac{\partial E_\varphi}{\partial r}\right) \tag{14}$$

By Eqs. (12) and (14), we can obtain the vertical magnetic field response in the four layered medium.

3 Analysis of propagation effects

The propagation of electromagnetic waves in a homogeneous medium may produce amplitude attenuation and phase shift. In a non-uniform medium, due to the presence of interface, it may cause reflection, refraction or transmission, i.e. propagation effects. When the electric field is perpendicular to the incident surface, the direction relations of the incident wave vector k_i, reflected wave vector k_r and transmitted wave vector k_t are shown in Fig. 3, where n is the unit vector in the direction normal to the interface. The angles constituted by three wave vectors k_i, k_r, k_t and the normal are the angles of incidence, reflection and transmission θ_i, θ_r, θ_t, respectively. Incident and reflected waves propagate in the medium I, and the refracted wave propagates in the medium II. The wave number of medium is decided by the medium nature, namely:

$$\begin{cases} |k_i| = |k_r| = k_1 = \sqrt{\omega^2\varepsilon_1\mu_1 - i\omega\mu_1\sigma_1} \\[2mm] |k_t| = k_2 = \sqrt{\omega^2\varepsilon_2\mu_2 - i\omega\mu_2\sigma_2} \end{cases} \tag{15}$$

By Snell's law, we obtain the relationships of reflected wave electric field E_r, transmitted wave electric field E_t and incident wave electric field E_i as follows:

$$E_r = \frac{\mu_2\xi_1 - \mu_1\xi_2}{\mu_2\xi_1 + \mu_1\xi_2}E_i \tag{16}$$

$$E_t = \frac{2\mu_2\xi_1}{\mu_2\xi_1 + \mu_1\xi_2}E_i \tag{17}$$

Then the reflection coefficient of the electromagnetic wave in the interface of medium I and medium II becomes:

$$r_{TE} = \frac{\mu_2\xi_1 - \mu_1\xi_2}{\mu_2\xi_1 + \mu_1\xi_2} \tag{18}$$

where, $\begin{cases} \xi_1 = k_1\cos\theta_i \\ \xi_2 = k_2\cos\theta_t = \sqrt{k_2^2 - k_1^2\sin^2\theta_i} \end{cases}$.
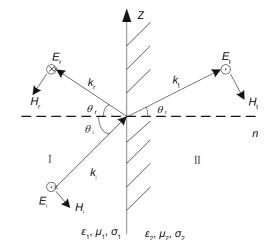

Fig. 3 The direction of electric field perpendicular to the incidence plane

If there are multiple interfaces in the medium, the electromagnetic wave may undergo multiple reflection and refraction. For the condition of two interfaces, the propagation of electromagnetic waves is shown in Fig. 4. It can be seen that in medium II, there are not only the transmitted wave but also the reflected wave. In addition, when the transmitted wave from medium I to medium II reaches the second interface, it becomes the incident wave from medium II to medium III. When the reflected wave from medium III to medium II reaches the first interface, it becomes the incident wave from medium II to medium I. The above analysis shows that in addition to the direct wave, there are also reflection, reflection-transmission and multiple reflection-transmission waves in received signals. So we are unable to accurately describe wave components as incident wave, reflected wave and refracted wave. In order to describe the field of layered homogeneous medium with axial symmetry, the cylindrical inward and outward wave functions are needed. In Eq. (12) A_1, A_2, A_3 represent the inward wave coefficients of mandrel, borehole and casing, respectively, and B_2, B_3, B_4 represent their outward wave coefficients. By the continuity conditions of the tangential component of the electric and magnetic fields in a cylindrical layered medium in a borehole, we can obtain the required coefficients.

4 Numerical calculation of propagation effects

4.1 Eddy current loss within the mandrel

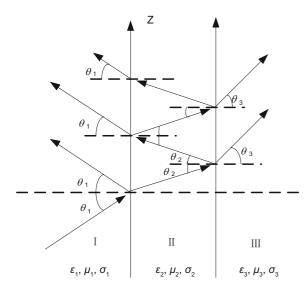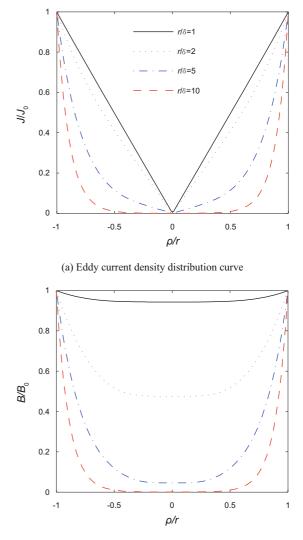A coil wound around a mandrel is a commonly used form of emission source in electromagnetic detection. With

Fig. 4 The multiple reflection and refraction of electromagnetic waves

(a) Eddy current density distribution curve

(b) Magnetic flux density distribution curve

Fig. 5 The distribution curve of eddy current and magnetic flux along the mandrel radial direction

a conductive mandrel, the ring current source may generate eddy currents in the mandrel, thereby causing eddy loss. As reflection and refraction of electromagnetic waves do not exist within the mandrel, the attenuation characteristics of electromagnetic waves in it can be represented by the skin depth $\delta = \sqrt{2/\omega\mu_1\sigma_1}$. For different r/δ, Fig. 5 gives the curves of J/J_0 and B/B_0 changing with ρ/r inside the mandrel. J_0 and B_0 are the eddy current density and magnetic flux density on the mandrel surface. r is the mandrel radius and ρ is the radial distance from the axis to field point within the mandrel. It can be seen that the distribution of eddy current density and magnetic flux density along the radial direction of the mandrel is very uneven. When r is fixed, the higher the transmitted frequency, the smaller the skin depth of electromagnetic waves in the mandrel, the greater the value r/δ. The uneven distribution of eddy current and magnetic flux within mandrel is more serious. This result indicates that the high frequency electromagnetic wave and the eddy induced by it can only reach a very thin surface of the mandrel, and the eddy current loss within the mandrel is proportional to the transmission frequency and mandrel conductivity. When ω and σ_1 are fixed, the smaller r, the smaller r/δ. The distribution of eddy current and magnetic flux within mandrel is more uniform. That is, the eddy current loss within the mandrel is proportional to the mandrel radius.

4.2 Field within the mandrel

As the borehole is the active region, the fields in the borehole include the field in the uniform medium, the outward wave component of mandrel and the inward wave component of the borehole. The mandrel is a passive region, so the field within it is only the outward wave component of the mandrel. First, we analyze the influence of the coil vertical offset on the electromagnetic response in the mandrel. We take the vertical offset between two coils z =0.1, 0.3, 0.6, 1.0 m, respectively. The variation curves of the electromagnetic response with the mandrel conductivity are shown in Fig. 6. Fig. 6(a)

represents the real part of the electric field response within the mandrel, Fig. 6(b) represents the real part of the magnetic field response, Fig. 6(c) represents the imaginary part of the electric field response and Fig. 6(d) represents the imaginary part of the magnetic field response. The simulation results show that the electromagnetic responses within the mandrel rapidly reduce with an increase of mandrel conductivity. When the conductivity further increases, the electromagnetic responses gradually approach zero. It also indicates that the higher the mandrel conductivity, the larger the losses inside the mandrel. If the mandrel is an ideal conductor, there is no field within the mandrel. In addition, the smaller the vertical offset between the transmitting coil and receiving coil, the higher the amplitude of the electromagnetic field response in the mandrel. This can be interpreted as the density of magnetic field lines within the mandrel reduces with the increase of the vertical offset, resulting in decrease of the electromagnetic response amplitude.

Next, we discuss the impact of mandrel radius on its internal electromagnetic response. We take the mandrel radius r=35, 40, 45, 50 mm, respectively, and the mandrel
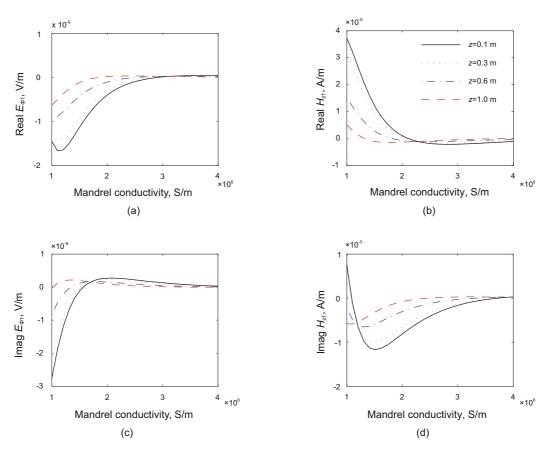
Fig. 6 The impact of coil vertical offset on the electromagnetic field response in the mandrel

conductivity is increased from 1×10^6 to 5×10^6 S/m. The electromagnetic response curves of different mandrel radii are shown in Fig. 7. For a larger mandrel radius, the electromagnetic field responses within it become lower. The smaller the mandrel radius, the lower the eddy current loss within the mandrel, so the eddy current loss within the mandrel is proportional to its radius. In addition, electromagnetic responses decrease rapidly with the increase of the mandrel conductivity and gradually approach zero. This again proves that there is no electromagnetic field inside a perfect conductor and eddy current loss within the mandrel is proportional to the mandrel conductivity.

4.3 Field in the formation

As the formation is a passive region in Fig. 1, the field in the formation only includes the outward wave component of the casing. By the above discussion, we know that when electromagnetic waves enter a conductor, due to skin effect, electromagnetic waves and the induced eddy can only penetrate a very thin surface of the conductor. The penetration depth is dependent on transmission frequency, medium conductivity and medium permeability. In order to make the electromagnetic waves enter the formation, the penetration depth in the casing must be greater than the casing thickness. In fact, if the casing is an ideal conductor ($\sigma_3 \rightarrow \infty$), then $k_3 \rightarrow i\sqrt{i}\infty$ according to Eq. (15). The electromagnetic wave reflection coefficient at the inner casing can be obtained by taking the limit of Eq. (18), i.e. $|r_{TE}|=1$. At this time,

electromagnetic waves produce total reflection. So the metal conductor has a serious shielding effect on electromagnetic signals (especially high frequency electromagnetic waves), and electromagnetic waves in an ideal conductor can not penetrate the conductive medium.

The penetration depth of electromagnetic waves within the casing is dependent on the transmission frequency when the casing material is fixed. We choose iron ($\sigma=1.0\times10^7$ S/m, μ_r=1000), aluminum ($\sigma=3.5\times10^7$ S/m, μ_r=1), copper ($\sigma=5.8\times10^7$ S/m, μ_r=1), and nickel ($\sigma=1.0\times10^7$ S/m, μ_r=600) as the casing material, respectively. The transmission frequency is increased from 0.01 to 100 Hz. Fig. 8 shows the electromagnetic response curves of different casing materials. Fig. 8(a) shows the real part of the electric field response in the formation when the mandrel conductivity σ_1=2,000,000 S/m, Fig. 8(b) shows the real part of the electric field response when σ_1=4,000,000 S/m and Fig. 8(c) shows the real part of the electric field response when σ_1=6,000,000. Fig. 8(d), Fig. 8(e) and Fig. 8(f) correspond to the imaginary part of the electric field response in the formation of different mandrel conductivity. The electric field response in the formation of an open hole is significantly higher than that of a cased hole. For the metal casing, the lower the transmission frequency, the more easily the electromagnetic signals penetrate the casing. This proves that the casing has serious shielding effect on electromagnetic signals. Furthermore, for the cased hole, the peak of the electric field response corresponds to a transmission frequency f =1 Hz. When the
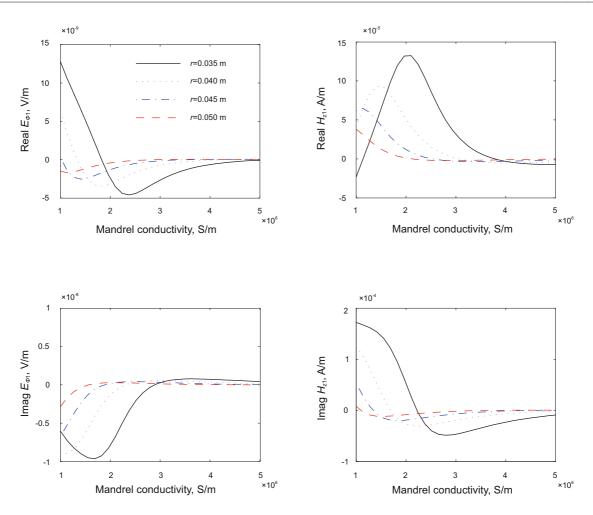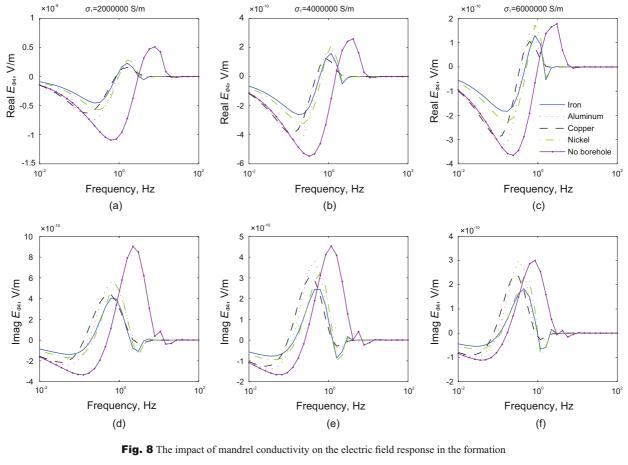
Fig. 7 The impact of mandrel radius on the electromagnetic field response in the mandrel

borehole is uncased, this peak is f =10 Hz. So we should select the transmitted signal in the lower frequency range to make electromagnetic waves penetrate the casing. Comparing Fig. 8(a) with Fig. 8(b) and Fig. 8(c) or comparing Fig. 8(d) with Fig. 8(e) and Fig. 8(f), we can see that the electric field response amplitudes in the formation reduce with an increase of mandrel conductivity. The higher the mandrel conductivity, the greater the eddy current loss within the mandrel and the weaker the electromagnetic signals penetrating casing.

We select iron, aluminum, copper, and nickel as the casing material and the transmitted frequency is increased from 0.01 to 100 Hz. The electromagnetic response curves of different casing materials are shown in Fig. 9. Fig. 9(a) shows the real part of the electric field response in the formation when the mandrel relative permeability μ_{1r} = 200, Fig. 9(b) shows the real part of the electric field response when μ_{1r} = 300 and Fig. 9(c) shows the real part of the electric field response when μ_{1r} = 400. Fig. 9(d), Fig. 9(e) and Fig. 9(f) correspond to the imaginary part of the electric field response in the formation of different mandrel relative permeabilities. The results indicate that the real and imaginary parts of the electric field response of a cased hole are lower than those of an open hole. When the transmission frequency is close to 1 Hz, the electromagnetic waves can easily enter the formation through the metal casing. In addition, comparing Fig. 9(a)

with Fig. 9(b) and Fig. 9(c) or comparing Fig. 9(d) with Fig. 9(e) and Fig. 9(f), we can see that the electric field response amplitudes reduce with an increase of mandrel relative permeability. The higher the mandrel relative permeability, the greater the eddy current loss within the mandrel, and the weaker the electromagnetic signals in the formation.

In the following, we discuss the impact of casing physical parameters on the response signals in the formation. The casing thickness is fixed as $\Delta r = r_2 - r_1 = 3$, 6, 9, 11 mm, respectively. Then, the transmission frequency is increased from 0.01 to 100 Hz. Fig. 10 shows the response curves of different casing thickness. The simulation results show that the thicker the casing, the lower the response signal amplitudes. The electromagnetic signal has more difficulty penetrating the casing with an increase of transmission frequency, making the response signals reduce rapidly and eventually approach zero. With an increase of the casing thickness, the transmission frequency corresponding to the peak of response signals gradually moves to the left direction of the frequency axis. For example, when the casing thickness $\Delta r = 3$ mm, the peak is corresponding to the transmission frequency close to 5 Hz. When $\Delta r = 11$ mm, the peak is corresponding to the frequency close to 1 Hz. Therefore, the transmission frequency should be adjusted with the change of casing thickness in order to make the electromagnetic signals
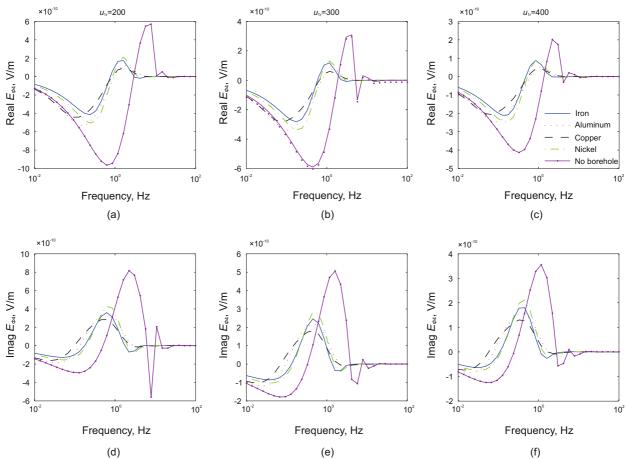
Fig. 8 The impact of mandrel conductivity on the electric field response in the formation

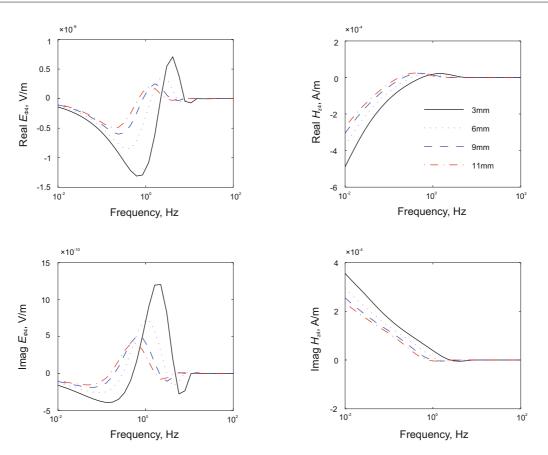**Fig. 9** The impact of mandrel permeability on electric field response in the formation

Fig. 10 The impact of casing thickness on the electromagnetic response in the formation
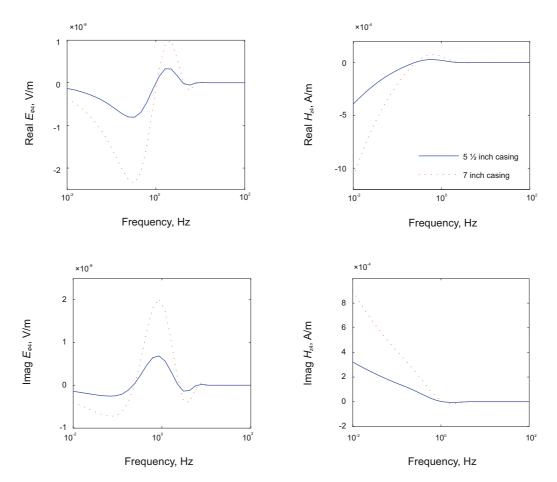
Fig. 11 The impact of casing diameter on the electromagnetic response in the formation

penetrate the casing easily.

We also compute the electromagnetic responses of 5½ inch casing and 7 inch casing. The response curves of different casing diameters are shown in Fig. 11. The figure shows that when the casing thickness remains unchanged, the larger the casing diameter, the higher the response signal amplitudes. This phenomenon can be interpreted as the casing with small diameter is equivalent to a limit to magnetic field lines. The decrease of magnetic field lines entering the formation resulting in a decrease of signal response amplitudes. So we can infer that as long as the casing thickness remains unchanged, the skin depth required for the electromagnetic signal penetrating the casing is the same, and the transmission frequency remains unchanged as well.

5 Conclusions

In the propagation of electromagnetic waves in a layered uniform conductive medium, there are not only amplitude attenuation and phase shift, but also reflection and refraction caused by the presence of the interfaces, i.e., propagation effects. According to the basic electromagnetic theory, we establish a mathematical model of low-frequency electromagnetic logging methods in a production well. The general expressions of electromagnetic response in a uniform conductive medium or a layered lossy medium are derived by the geometry relationship of the ring current source around the mandrel. The propagation effects produced by low-frequency electromagnetic waves in a cylindrical layered medium are also discussed in detail. The simulation results of eddy current density and magnetic flux density along the radial direction of mandrel show that the eddy current loss is proportional to the mandrel conductivity and the transmission frequency. The numerical results of different vertical offsets between sending and receiving coils or the mandrel radius indicate that both of the two parameters have a significant influence upon the electromagnetic responses within the mandrel. The frequency response characteristics of different physical and electrical parameters of the casing show that the casing thickness has an important impact on the selection of the transmission signal frequency. It is also discovered that the effect of the casing diameter can be ignored. The numerical analysis of propagation effects of low-frequency electromagnetic waves in a cased hole and the discussion of the frequency response characteristics of the secondary field lay a good foundation for identifying the medium outside the casing. This is significant for forward modeling, inversion and data interpretation of the low-frequency electromagnetic method.

Acknowledgements

References

Askey S, Farag S, Logan J, et al. Cased hole resistivity measurements optimize management of mature waterflood in Indonesia. SPWLA 43rd Annual Logging Symposium. 2002. 6: 2-5

Bao D Z, Cheng X, Liu J, et al. Development of the TCFR-09 cased hole resistivity logging detector. Well Logging Technology. 2010. 34(5): 473-475 (in Chinese)

Che X H and Qiao W X. Numerical simulation of an acoustic field generated by a phased arc array in a fluid-filled borehole. Petroleum Science. 2009. 6(3): 225-229

Fondyga A, Ecuador Q, Sherba G, et al. Cased hole density, neutron, sonic and resistivity logging in South America, case histories, lessons learned, and a methodology for including the technology in formation evaluation programs. SPWLA 45th Annual Logging Symposium. 2004. 6: 6-9

Gao J, Liu F P, Bao D Z, et al. Study on forward modeling of through-casing resistivity logging. Science in China Series D: Earth Sciences. 2008a. 51(Suppl): 207-211 (in Chinese)

Gao J, Liu F P, Bao D Z, et al. Responses simulation of through-casing resistivity logging in heterogeneous-casing wells. Chinese Journal of Geophysics. 2008b. 51(4): 1255-1261 (in Chinese)

Kang J Z, Xing G L and Yang S D. A study on the two-dimensional full-parameter inversion method of the electromagnetic propagation resistivity logging. Chinese Journal of Geophysics. 2006. 49(1): 275-283 (in Chinese)

Kaufman A A. The electrical field in a borehole with a casing. Geophysics. 1990. 55(1): 29-38

Kaufman A A and Wightman W E. A transmission-line model for electrical logging through casing. Geophysics. 1993. 58(12): 1739-1747

Schenkel C J and Morrison H F. Electrical resistivity measurement through metal casing. Geophysics. 1994. 59(7): 1072-1082

Shen J S and Sun W B. 2.5-D modeling of cross-hole electromagnetic measurement by finite element method. Petroleum Science. 2008. 5(2): 126-134

Song X J, Dang R R, Guo B L, et al. Research on transient electromagnetic response of magnetic source in borehole. Chinese Journal of Geophysics. 2011. 54(4): 1122-1129 (in Chinese)

Vail W B. Methods and apparatus for measurement of the resistivity of geological formation from within cased well in presence of acoustic and magnetic energy sources. U.S. Patent No. 5043669. August 27, 1991

Vail W B. Measuring resistivity changes from within a first cased well to fluids injected into oil bearing geological formation from a second cased well while passing electrical current between two cased well. U.S. Patent No. 5187440. February 16, 1993a

Vail W B. Methods of operation of apparatus measuring formation resistivity from within a cased well having one measurement and two compensation steps. U.S. Patent No. 5223794. June 29, 1993b

Wang Z G. Study on the Russian through-casing resistivity logging and its application. Well Logging Technology. 2009. 33(4): 374-378 (in Chinese)

Xu W and Habashy T M. Influence of steel casings on electromagnetic signals. Geophysics. 1994. 59(3): 378-390

Xue G Q, Li X, Guo W B, et al. Equivalent transformation from TEM field sounding data to plane-wave electromagnetic sounding data. Chinese Journal of Geophysics. 2006. 49(5): 1539-1545 (in Chinese)

(Edited by Hao Jie)